

# 論文 Finite Element Analysis of Steel Girder-concrete Pier Composite Connection with Applications of Interface Elements

Chakree BAMRUNGWONG<sup>\*1</sup>, Atsuhiko MACHIDA<sup>\*2</sup>,  
Toshihiko NAGATANI<sup>\*3</sup>, and Toru SATO<sup>\*4</sup>

**ABSTRACT:** A distinct analytical methodology is proposed to closely simulate the real mechanical behavior of the structure consisting of steel girder-concrete pier composite connection with the emphasis on the newly developed interface elements connecting concrete to reinforcing bar and steel plate elements. The structure analyzed in this research is the one in the series of prototype specimens tested by Japan Highway Corporation and Construction Companies [1].

**KEYWORDS:** steel girder-concrete pier composite connection, finite element analysis, interface element

## 1. INTRODUCTION

According to the benefits on an improvement in structural performances, many continuous highway bridges consisting of steel girder-concrete pier composite connection have been constructed. However with a currently limited knowledge, to guarantee the load carrying capacity of such a structure, the load tests of the prototype specimens have to be conducted which is not cost effective and quite time consuming. In this paper, a rational finite element analytical methodology is proposed. The emphasis is paid on the development of the interface elements used to link concrete to steel plate and concrete to reinforcing bar elements. The reliability of this distinct analytical methodology is verified by comparing the results to those obtained from experiment. Then by this analytical methodology, the pattern of the stress distribution within the connection part is predicted.

## 2. ANALYTICAL METHODOLOGY

### 2.1 FINITE ELEMENT MODELING OF THE STRUCTURE

As the structure analyzed in this research was symmetric at the middle plane (z-x plane), a half structural model was constructed with the fixed displacement (in y-direction) and rotation (in about x- and z-axes) boundary conditions applied on the cutting plane. In order to separately account for the effects of each structural component, the structural model was discretely meshed. The structural components, those are, concrete, reinforcing bar, steel plate, and stud, were represented individually by the different types of element. The 8-node hexagonal elements were used to simulate the concrete material. The reinforcing bars including both stirrups and longitudinal ones, were represented by 2-node truss elements while 4-node thick shell elements were used to simulate the steel plate, and the

---

\*<sup>1</sup> Department of Civil and Environmental Engineering, Saitama University

\*<sup>2</sup> Department of Civil and Environmental Engineering, Saitama University

\*<sup>3</sup> Research Division, Japan Highway Corporation

\*<sup>4</sup> Research Division, Miyaji Iron Work Corporation

2-node beam elements were used to represent the studs. In this analysis, the interface elements modeled by springs, were used to connect concrete to reinforcing bar elements. As well, to take into consideration the effect of the stress transfer and the corresponding strain at the interface between concrete and steel plate elements, the spring element was used to link these two materials together. Every particular element was then given a unique constitutive law. Identically to the experiment, the constant downward pressure of magnitude 0.5 MPa was continuously imposed on the top of the pier from the beginning of analysis throughout the loading steps. The monotonic horizontal load was incrementally applied at the point 200 mm below the top of the pier. The detailed design and finite element meshes of the specimen considered in the analysis are as shown in Fig.1 and 2, whereas, the properties of materials are as shown in Table 1.

Table I Properties of materials

Material Properties	Concrete	Reinforcing Bar	Steel Plate
Modulus of Elasticity(MPa)	22,978	187,866	208,282
Compressive Strength(MPa)	31.03	-	-
Yield Strength(MPa)	-	373.8	297.2
Splitting Strength(MPa)	2.39	-	-

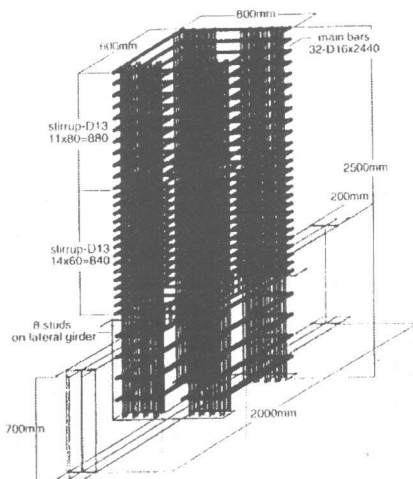


Fig.1 Detailed design of the specimen

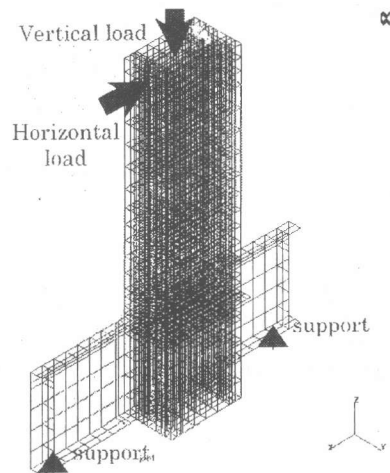


Fig.2 Finite element meshes

## 2.2 MATERIAL MODELING

After the finite element mesh was built up, the constitutive laws describing material characteristics were assigned to all elements. In the analysis, a simple elastic-perfectly plastic constitutive relationship is applied to all metallic components such as steel plate, reinforcing bar, and stud. For the concrete element, under compressive stress, the constitutive law was adopted from the experimental results. Under tensile stress, the concrete was assumed to behave elastically until reaching the tensile strength. Beyond this point, the concrete element would be cracked. Therefore, the tensile resistance of the element in the direction normal to the crack plane was assumed to drop down to zero.

## 2.3 DEVELOPMENT OF THE INTERFACE ELEMENTS

Since, in reality, the concrete is bonded to the reinforcing bar as well as to the steel plate, to simulate this situation in the analysis, the interface springs with the unique constitutive laws are used to link the concrete elements to the adjacent reinforcing bar and steel plate elements.

### 2.3.1 Interface between concrete and reinforcing bar elements

The properties of the interface between concrete and reinforcing bar proposed by Shima [2] was

adopted in this research as it was proved to be sufficiently generalized. Based on his experimental results, Shima derived the unique bond stress-slip-strain relationship which is as expressed in Eq.1.

$$\tau = \frac{0.73fc'(\ln(1+5s))^3}{1+\varepsilon \times 10^5} \quad (1)$$

where  $s = 1000S/D$ ,  $\tau$  = average bond stress,  $fc'$  = concrete strength,  $S$  = slip,  
 $D$  = bar diameter,  $\varepsilon$  = strain

However, in his research, Shima had not proposed any dedicated element to work with this constitutive law for the analysis with finite element method. Therefore, in order to apply this interface property in finite element analysis an interface element consisting of springs in 3 directions was developed in this research. In addition, as the bond stress derived by Shima is an average value which is not the stress occurs exactly at the surface of the reinforcing bar, thus in the analysis with the proposed interface elements linking the reinforcing bar to the adjacent concrete element, the location away from reinforcing bar surface where bond stress has an average value needs to be determined and the surface area at this location must be used in computing the average spring force and stiffness. The average spring force, or the bond force, can be determined by multiplying the average bond stress (Eq.1) with the bond-effective area as shown in Eq.2.

$$\text{Average bond force } (F_{\text{avg}}) = \tau \times k_z \pi D L \quad (2)$$

where  $k_z$  = bond-effective zone factor,  $L$  = length of the reinforcing bar element

By substituting the average bond stress ( $\tau$ ) from Eq.1 into Eq.2, and differentiating the average bond force ( $F_{\text{avg}}$ ) in Eq.2 with respect to slip while the strain in reinforcing bar is kept constant, the average spring stiffness can be found as expressed in Eq.3

$$K_{\text{avg}} = \frac{0.73fc' \times k_z \pi D L}{1 + \varepsilon \times 10^5} \times \left( \frac{15}{D + 5S} \right) \times \left( \ln \left( 1 + 5 \frac{S}{D} \right) \right)^2 \quad (3)$$

where  $K_{\text{avg}}$  = average stiffness of the interface spring in axial direction of reinforcing bar

In order to determine the location where the average bond stress acts upon, it is assumed that at the moment the concrete starts to crack, the reinforcing bar section located on that crack plane yields immediately. Based on this assumption, the maximum surrounding concrete area ( $A_{\text{cmax}}$  in Fig.3) that initiates this phenomena can be calculated as,  $A_{\text{cmax}} = [A_s \times f_y] / f_t$ , where  $A_s$  = sectional area of reinforcing bar,  $f_y$  = yield stress of reinforcing bar, and  $f_t$  = cracking stress of concrete. This derivation is similar to the calculation introduced by An., X et al. [3]. Furthermore, if this maximum surrounding concrete area is assumed to be of round shape and the bond stress distribution in radial direction from the reinforcing bar axis is assumed to be of triangular shape as shown in Fig.4, the surface area that the average bond stress acts upon will be larger than the surface of the reinforcing bar on where the interface element exists by the ratio  $k_z$  (bond-effective zone factor) as shown in Eq.4. By substituting the bond-effective zone factor into Eq.3, the average stiffness for interface spring that is necessary in the analysis, can be calculated.

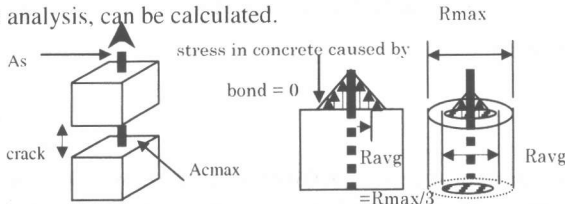


Fig.3 Sudden yielding of reinforcing bar on crack plane

Fig.4 Stress distribution within bond-effective zone

$$k_z = R_{\text{avg}} / R_{\text{bar}} = \frac{1}{3} \sqrt{\frac{f_y}{f_t}} \quad (4)$$

where  $R_{\text{avg}}$  = distance from the axis of reinforcing bar to the surface where average bond stress acts upon,  $R_{\text{bar}}$  = radius of the reinforcing bar.

### 2.3.2 Interface between concrete and steel plate elements

In this research, the concrete-steel plate interface property proposed by Yonezawa [4] was adopted because of its accuracy and simplicity in application. Even though Yonezawa had also developed the hexagonal-shaped interface element to be used in his finite element analysis, it was compulsory to assume the virtual thickness of the interface element. This somehow laterally initiated the ambiguity in the applicability of his element. In this work, the new interface element consisting of 3 springs linking concrete and steel plate nodes in 3 directions was proposed. With the newly developed element, the virtual thickness factor in Yonezawa's formulation was correspondingly normalized. This was done accordingly to the fact that the spring element possesses no thickness, or in other words, is dimensionless. Thus the problem in assigning an unclear value for virtual thickness could be eliminated. The formulation for the concrete-steel plate interface property and the derivation of the stiffness of such an interface element are as illustrated in Fig.5 and Table2, respectively.

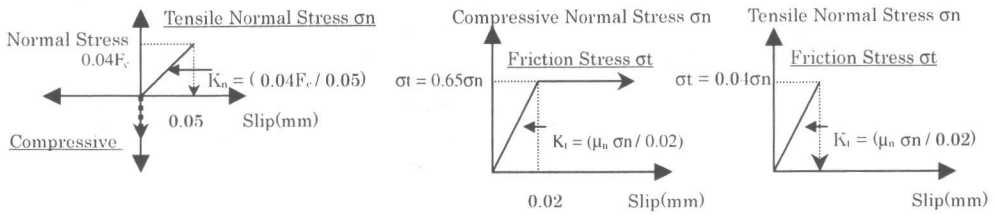


Fig.5 Stress-slip relationship of the interface element

Table2 Derivation of the stiffness of the concrete-steel plate interface element

Springs in the direction normal to the interface	Springs in the direction tangential to the interface
<p>1. Under compressive normal stress Assuming that under compressive stress, the interface is as rigid as steel plate, thus <math>K_n = (200,000A)</math> per unit length</p> <p>2. Under tensile normal stress <math>\sigma_n = (0.04 F_c / 0.05)\delta</math> <math>\sigma_n (A) = (0.04 F_c / 0.05)A\delta</math> <math>F_n = (0.04 F_c / 0.05)A\delta</math> Thus the stiffness of spring in this direction is <math>K_n = (0.04 F_c / 0.05)A</math></p> <p>Where <math>\sigma_n</math> : stress in the direction normal to the interface (<math>N/mm^2</math>), <math>F_c</math> : compressive strength of concrete (<math>N/mm^2</math>), <math>A</math> : effective area (<math>mm^2</math>), <math>F_n</math> : force in the direction normal to the interface (N), <math>\delta</math> : slip (the deformation of the spring, mm), <math>K_n</math> : Stiffness of spring in the direction normal to the interface (<math>N/mm</math>)</p>	<p>1. Under compressive normal stress [when; <math>\sigma_t \leq 0.65\sigma_n</math>] <math>F_t = (\mu_n \sigma_n / 0.02)A\delta</math> <math>K_t = (\mu_n \sigma_n / 0.02)A</math></p> <p>[when; <math>\sigma_t \geq 0.65\sigma_n</math>] assuming that the stress keeps constant while slip increases infinitely <math>F_t = 0.65 \sigma_n A</math> <math>K_t = 0</math></p> <p>2. Under tensile normal stress [when; <math>\sigma_t \leq 0.04\sigma_n</math>] <math>F_t = (\mu_n \sigma_n / 0.02)A\delta</math> <math>K_t = (\mu_n \sigma_n / 0.02)A</math></p> <p>[when; <math>\sigma_t \geq 0.65\sigma_n</math>] <math>F_t = 0</math> <math>K_t = \infty</math></p> <p>Where <math>F_t</math> : force in the direction tangential to the interface (N), <math>K_t</math> : stiffness in the direction tangential to the interface (<math>N/mm</math>)</p>

### 3. ANALYTICAL RESULTS

From the finite element analysis, the analytical results obtained can be shown in terms of load-displacement relationship, load-bar strain relationship, and the relationship between the load and principal strains on the web of the main girder (Fig.6). The good agreement could be observed when compared to the experimental results. Moreover, the plot between load and the principal strains

illustrates that with the application of the concrete-steel plate interface element, the change in strain due to the slip between the concrete and the steel girder could be predicted more accurately.

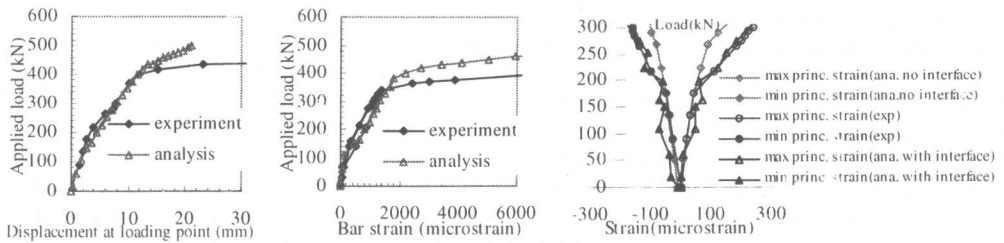


Fig.6 Relationship between applied load and displacement at the loading point, 200 mm below the top (left), relationship between load and the axial strain in reinforcing bar located at 50 mm above the top flange of the girder (middle), and relationship between load and principal strain at the center of the girder's web (right)

Fig.7 shows not only the distribution of the normal reaction forces on concrete elements placed at the faces named SIDE A1, A2, A3, and A4 (the reaction forces that equilibrate the forces exerted on concrete element by the surrounding elements adjacent to the faces being considered), but also points up that compared to the sections located farther from the main girder (C, D, and E), the stresses on the sections located at the vicinity of girder's flange (A and B) are greater. Therefore, it can be deduced that, in this type of specimen, the force transferred from the girder is not well spread throughout the reinforced concrete part in the connection. In the real structure, where the width of the concrete pier is much larger than the width of the girder's flange, in case that the magnitude of forces applied to the girder is excessively high, this stress concentration may cause a local deterioration to the concrete situated near the flanges of the girder.

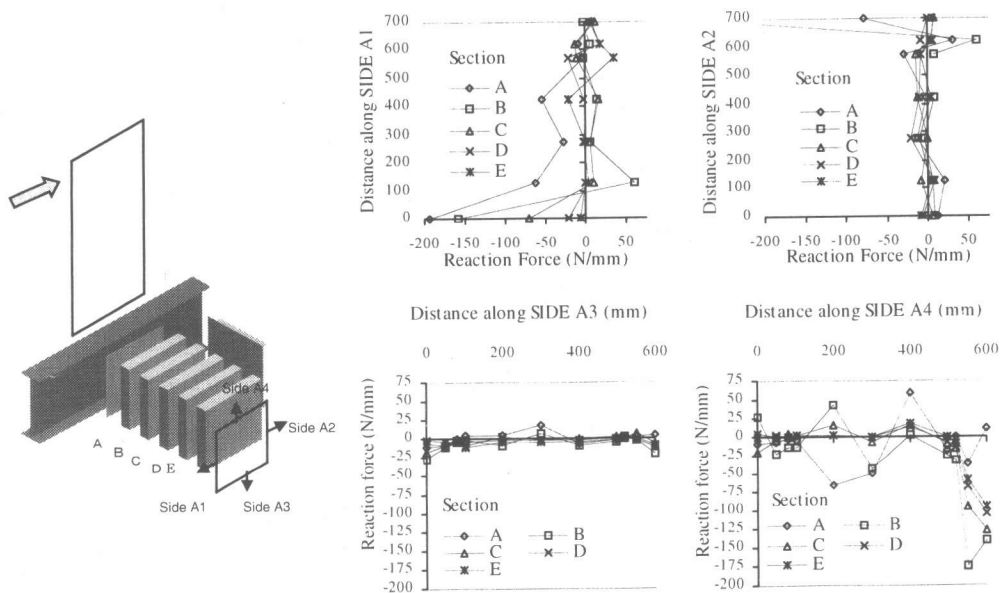


Fig.7 Distribution of the normal reaction force on concrete sections within the connection part

#### 4. CONCLUSIONS

1. With the proposed analytical methodology the behavior of structure consisting of steel girder-concrete pier composite connection can be closely simulated.
2. The application of the concrete-steel plate interface elements helps improve the accuracy of the analysis. As well, the application of concrete-reinforcing bar interface element can be considered to be the alternative method to predict the behavior of reinforced concrete in addition to the application of smeared crack concept that was regarded to be not sufficiently generalized for the finite element analysis of this type of composite structure [5].
3. The design of the bridge structure consisting of steel girder-concrete pier composite connection should be rigorously performed with taking into consideration that the stress will be well distributed throughout the connection so that the local deterioration of concrete can be avoided.

#### REFERENCES

1. Japan Highway Corporation, "Experimental Investigation of The Behavior of Steel Girder-Concrete Pier Rigid Connection Type-1B", Interim Report, December 1998.
2. Shima, H., "Micro and Macro Models for Bond Behavior in Reinforced Concrete", Doctor of Engineering Dissertation, The University of Tokyo, December 1986.
3. An, X. et al., "Numerical Simulation of Size Effect in Shear Strength of RC Beams", J. Materials Conc. Struct., Pavements, JSCE, No.564, Vol.35, pp. 297-316, May 1997.
4. Yonezawa, K., "Development of Nonlinear Finite Element Analysis for Structural Concrete Member and Its Shear Resistance Mechanism", Doctor of Engineering Dissertation, Chiba University, March 1995.
5. Bamrungwong, C. et al., "Finite Element Analysis of Steel Girder-Concrete Pier Rigid Connection", Transactions of The Japan Concrete Institute, Vol.22, pp. 331-336, 2000.